CMS Physics Analysis Summary

Contact: cms-phys-conveners-ftr@cern.ch 2018/11/19

First Level Track Jet Trigger for Displaced Jets at High Luminosity LHC

The CMS Collaboration

Abstract

The CMS detector for the planned high luminosity LHC run will have a new first level (L1) hardware track trigger. The impact of the L1 track trigger is explored based on the potential increase of CMS sensitivity to signals beyond the standard model in final states with multiple jets and low total transverse energy. In particular, there is currently an blind spot for lifetimes of order 1 cm in searches for new long-lived scalars ϕ in Higgs decays, i.e. $\mathrm{H}(125) \rightarrow \phi\phi \rightarrow 4j$. It is found that a plausible extension of the L1 track trigger to tracks with an impact parameter of a few centimeters results in dramatic gains in the trigger efficiency. The gains are even larger for additional heavy SM-like Higgs bosons with the same decay.

1 Introduction

The high luminosity LHC program offers many exciting opportunities to search for rare processes. It is expected that the LHC will accumulate $3\,\text{ab}^{-1}$ of proton-proton (pp) collisions at 14 TeV. The CMS detector will undergo major upgrades to all subsystems, including the tracker [1], the barrel [2] and endcap [3] calorimeters, the muon system [4], and the trigger [5].

The bandwidth limitations of the first level (L1) trigger are one of the main problems facing current searches for exotic Higgs boson decays, as well as many other signals beyond the standard model (BSM). The Higgs boson is assumed to be SM-like within this document with the same production cross-sections as the observed Higgs boson, but including rare unobserved decays with $\mathcal{B} = 10^{-5}$. The process where the Higgs boson decays to two new light scalars that in turn decay to jets, $\text{H}(125) \rightarrow \phi\phi \rightarrow 4j$, is an important example. If the scalar ϕ has a macroscopic decay length, the offline analysis has no background from SM processes, but the majority of the signal events do not get recorded because they fail to be selected by the L1 trigger. The main obstacle is the high rate for low transverse momentum jets, which is made worse by additional extraneous pp collisions in the high luminosity environment.

In this note, we investigate the capabilities of L1 track finding [1] to increase the L1 trigger efficiency for such signals. We focus on small or moderate decay lengths of the new particles, 1–50 mm, and assume, as is demonstrated by many analyses [6–8], that the offline selection can remove all SM backgrounds with only a moderate loss of efficiency.

The investigation has two major thrusts. First, we propose a jet clustering algorithm that uses the L1 tracks found with a primary vertex constraint. Second, we consider the extension of the L1 track finder to off-pointing tracks, and develop a jet lifetime tag for tracks with $|\eta| < 1.0$. Off-pointing tracks do not point back to the primary collision point, but instead have a "kink" arising from the decay vertex of a long-lived decay. The kink is usually quantified in terms of the transverse impact parameter, d_0, which gives a measure of the smallest distance between the transverse projection of the track and the primary collision point. Future work will include: expanding the off-pointing track finding at L1 to the full acceptance of the outer tracker; matching the track jets with high transverse momentum (p_T) deposits in the electromagnetic calorimeter; and finding new ways to evaluate track quality to suppress "fake" tracks that result from finding the wrong combination of track hits.

While in this study we focus on the specific Higgs boson decay to light scalars (see Ref. [9] for extensive review of physics motivations for such decays), the results and the proposed triggers are relevant for a broad spectrum of new physics searches, with or without macroscopic decay lengths.

2 Signal and background simulation

In these studies, the Phase-2 CMS detector is simulated using GEANT4 [10]. Event samples corresponding to 200 collisions per bunch crossing (pileup) [5] are used for the evaluation of trigger rates.

The following signal samples are considered:

1. Displaced single muons, generated with a uniform distribution of transverse momentum (p_T) between 2 and 8 GeV, uniform in η between -1 and 1, and with impact parameter d_0 distributed as a Gaussian with width $\sigma = 2\,\text{cm}$.

2. The exotic decay of the SM-like Higgs boson $H(125) \to \phi\phi \to b\bar{b}b\bar{b}$, with ϕ masses of 15, 30, and 60 GeV, and $c\tau$ of 0, 1, and 5 cm. The production of the Higgs boson via gluon fusion is simulated by POWHEG v2.0 [11], while the hadronization and decay is performed by PYTHIA v8.205 [12].

3. The decay of a heavy SM-like Higgs boson with mass 250 GeV, $H(250) \to \phi\phi \to b\bar{b}b\bar{b}$, with ϕ masses of 15, 30, and 60 GeV, and $c\tau$ of 0, 1, and 5 cm. The production of the heavy SM-like Higgs boson via gluon fusion, its decay, and its hadronization are all simulated with PYTHIA v8.205 [12].

3 Track jets

The tracker is the most granular detector participating in the L1 decision, and therefore the most resilient to pileup. Track finding at L1 relies on selecting tracker hits that originate from high transverse momentum particles. This is achieved in the front-end electronics through use of the so-called p_T-modules, each consisting of two sensors separated by a few mm [1]. A particle crossing a tracker module produces a pair of hits in the two sensors. Such pairs form a "stub" if the azimuthal difference between the hits in the two sensors of a module is consistent with a prompt track with $p_T \gtrsim 2$ GeV.

In this section, we describe a simple jet clustering algorithm implementable in firmware, and compare it with anti-k_T jets [13] with a size parameter of $R = 0.3$, as produced by FASTJET [14].

3.1 Algorithm description

A simplified algorithm for L1 track jets is used to facilitate the firmware implementation for the L1 trigger applications. L1 track jets are found by grouping tracks in bins of z_0, the point of closest approach to the z-axis, for the tracks. The bins are overlapping, staggered by half a bin, so that each track ends up in two bins, eliminating inefficiencies at bin edges. In each z_0 bin, the p_T of the tracks are summed in bins of η and azimuthal angle ϕ with bin size 0.2×0.23. A simplified nearest-neighbor clustering is performed, and the $\sum p_T^{trk}$ in the z_0 bin is calculated. The z_0 bin with the highest $\sum p_T^{trk}$ is chosen. Jets obtained through this algorithm are referred to as "TwoLayer Jets." For the studies below, z_0 bins with size 6 cm are used. Jets with $p_T > 50\,(100)$ GeV are required to have at least two (three) tracks.

3.2 Track selection

The track purity depends on the number of stubs in the track and the χ^2 of the track fit. High-p_T tracks are much less pure than low-p_T tracks, with fake tracks distributed approximately uniformly in $1/p_T$ while real tracks are mostly low-p_T. To mitigate the effect of high-p_T fake tracks, any track with a reconstructed p_T above 200 GeV is assigned a p_T of 200 GeV. The track quality selection used in this analysis is summarized in Table 1.

Table 1: Track selection for jet finding. The χ^2 selections are per degree of freedom for a 4-parameter track fit.

track p_T	4 stubs	5 stubs	6 stubs
2–10 GeV	$\chi^2 < 15$	$\chi^2 < 15$	accept
10–50 GeV	reject	$\chi^2 < 10$	accept
>50 GeV	reject	$\chi^2 < 5$	$\chi^2 < 5$

3.3 Comparison with FASTJET

We have verified that the TwoLayer trigger algorithm gives similar performance to a full jet clustering using the anti-k_T algorithm with a size parameter $R = 0.3$, as implemented in FASTJET. Figure 1 shows the efficiency to reconstruct a track jet as function of the generator-level jet p_T. Figure 2 shows the calculated L1 trigger rates for an H_T trigger, computed as the scalar sum of p_T of jets. H_T is computed from track jets with $p_T > 5$ GeV. Figure 2 also shows the calculated L1 trigger rates for a quad-jet trigger with at least four track jets above a jet p_T threshold.

The rates are computed based on a fixed number of colliding bunches. The trigger rate is computed as

$$\text{Rate} = \epsilon^{\text{L1 Thresh}} N_{\text{bunches}} f_{\text{LHC}},$$

where $N_{\text{bunches}} = 2750$ bunches for 25 ns bunch spacing operation, $f_{\text{LHC}} = 11246$ Hz, and $\epsilon^{\text{L1 Thresh}}$ is the efficiency to pass a given L1 threshold as determined in simulation. For both the L1 trigger efficiency and rate, the performance of the TwoLayer hardware algorithm is compatible with the performance from the more sophisticated algorithm from FASTJET.

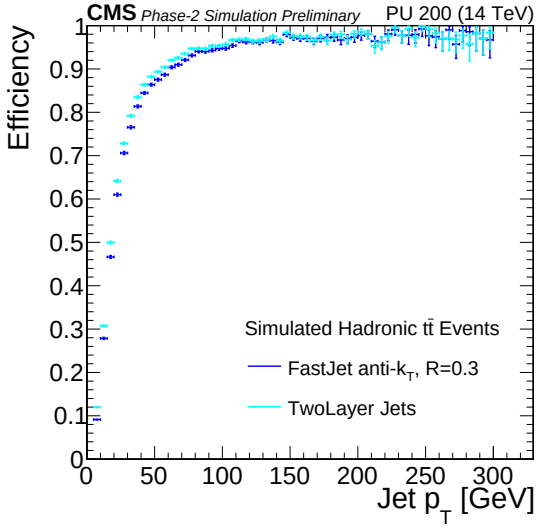

Figure 1: The efficiency for a jet to give rise to a L1 track jet as a function of the generator-level p_T of the jet. The light and dark blue lines correspond to the trigger clustering (TwoLayer Jets) and anti-k_T with $R = 0.3$ (FASTJET), respectively.

4 Displaced track finding

In this section, we briefly describe the performance of an algorithm for reconstruction of tracks with non-zero impact parameter. This approach extends the baseline L1 Track Trigger design to handle tracks with non-zero impact parameter and to include the impact parameter in the track fit. This enhanced design is feasible without greatly altering the track finding approach, but will require more FPGA computational power than the current proposal, which only considers only prompt tracks. Tracks passing the selection are clustered using the same algorithm as described in Section 3, and clusters containing tracks with high impact parameters are flagged as displaced jets. Though the baseline design of the L1 Track Trigger currently is optimized to find prompt tracks, these studies show that an enhanced L1 Track Trigger can extend the L1 trigger acceptance to include new BSM physics signals.

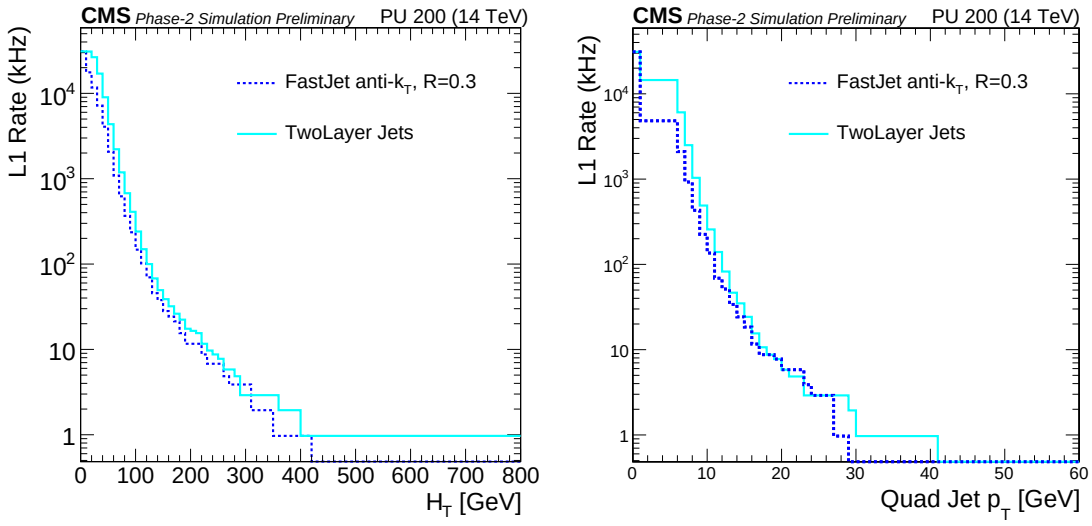

Figure 2: Calculated L1 trigger rates for track jet based H_T (left) and quad-jet (right) triggers. The light and dark blue lines correspond to the trigger clustering (TwoLayer Jets) and anti-k_T with $R = 0.3$ (FastJet), respectively.

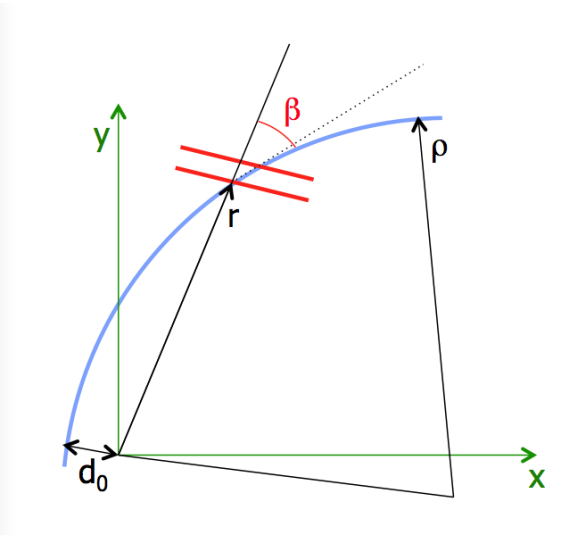

Figure 3: A sketch of a track crossing a p_T-module.

4.1 Stub efficiency

A track with a sufficiently small impact parameter can produce a stub. For tracks with large p_T (i.e. large curvature radius ρ) and small d_0, the bending angle β between the track and the prompt infinite momentum track, as shown in Fig. 3, is

$$\beta \approx \frac{r}{2\rho} - \frac{d_0}{r}.$$

Therefore, for a given d_0, one expects the stubs to be formed more efficiently as the radius of the module r increases. Fig. 4 shows the efficiency for a displaced muon to produce a stub as a function of the signed transverse momentum and the impact parameter of the muon, as measured in the full GEANT4-based simulation of the Phase-2 detector. After the first layer of the tracker the stub reconstuction efficiency is high across a range of impact paramters. In the first layer of the tracker there is some inefficiency for impact parameters above 2 cm. Fig. 4 shows that for a range of impact paramters the stub reconstruction efficiency is large.

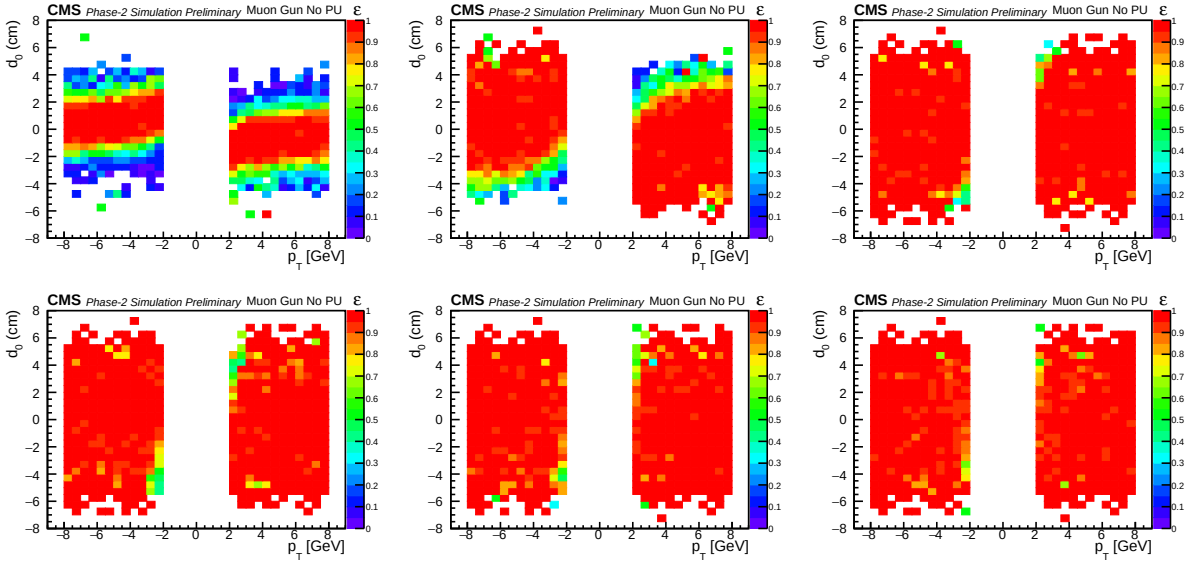

Figure 4: The efficiency for a displaced muon to form stubs in the six barrel layers of the Phase-2 tracker, as a function of the signed muon p_T and impact parameter. The top row shows, from left to right, layers 1, 2, and 3; the bottom row shows layers 4, 5, and 6. The sample is comprised of 2000 muons generated with uniformly distributed transverse momentum between 2 and 8 GeV and pseudorapidity $|\eta| < 1$, and with the impact parameter d_0 distributed as a Gaussian with width of 2 cm.

4.2 Track finding efficiency

A special version of the tracklet algorithm [1] has been developed that is capable of reconstructing tracks with impact parameters of a few cm. For now, the reconstruction is limited to the barrel region ($|\eta| < 1.0$). Preliminary feasibility studies show that the algorithm will have similar performance in the entire outer tracker coverage.

Fig. 5 shows the track reconstruction efficiency requiring at least four and at least five stubs on the track. As expected, allowing only four stubs on a track gives a higher efficiency for high impact parameter tracks. The five stub efficiency is large at high momentum with impact parameter less than 3 cm. The five stub tracks will have larger purity than the 4 stub tracks, which motives the selection defined in the next section.

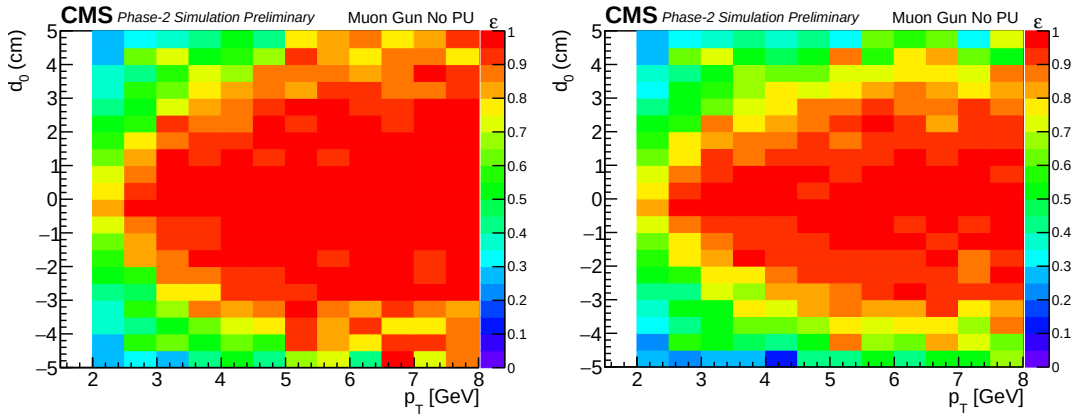

Figure 5: The efficiency for a displaced muon to be reconstructed as a track with at least four stubs (left) and at least five stubs (right).

4.3 Track selection

For the extended track finding algorithm, two track fits are performed: a 3-parameter $r\phi$ fit yielding $1/\rho$, ϕ_0, and d_0, and a 2-parameter rz fit yielding t and z_0. The bend consistency variable is defined as

$$\text{consistency} = \frac{1}{N_{\text{stubs}}} \sum_{i=1}^{N_{\text{stubs}}} \left(\frac{\beta_i - \beta_i^{\text{exp}}}{\sigma_i} \right)^2 ,$$

where N_{stubs} is the total number of stubs comprising the track, β_i and β_i^{exp} are the measured and expected bend angles for stub i, and σ_i is the expected bend angle resolution.

Two track categories are defined, loose and tight. The selection is summarized in Table 2.

Table 2: Track selection criteria for jet finding with extended L1 track finding.

	Loose			Tight		
N_{stubs}	$\chi^2_{r\phi}$	χ^2_{rz}	consistency	$\chi^2_{r\phi}$	χ^2_{rz}	consistency
4	<0.5	<0.5	<1.25	reject		
≥ 5	<5.0	<2.5	<5.0	<3.5	<2.0	<4.0

A jet is required to have at least two tracks passing the tight selection. If two or more tight tracks in a jet have $|d_0| > 0.1$ cm, the jet is tagged as a displaced jet.

5 Results

5.1 Track jets with prompt track reconstruction

Figure 6 shows the rate of the track jet H_{T} trigger as a function of the efficiency of the heavy SM-like Higgs boson signal. While for prompt ϕ decays one can realistically achieve 20% efficiency at an L1 rate of 25 kHz, the efficiency quickly drops with the decay length, since the displaced tracks are not reconstructed for d_0 values above a few mm.

5.2 Track jets with a displaced tag

The rate for the H_{T} trigger using the extended track finding is shown in Fig. 7, with and without a requirement of at least one jet with a displaced tag. The displaced tag requirement suppresses the rate by more than an order of magnitude. The displaced tracking and the trigger

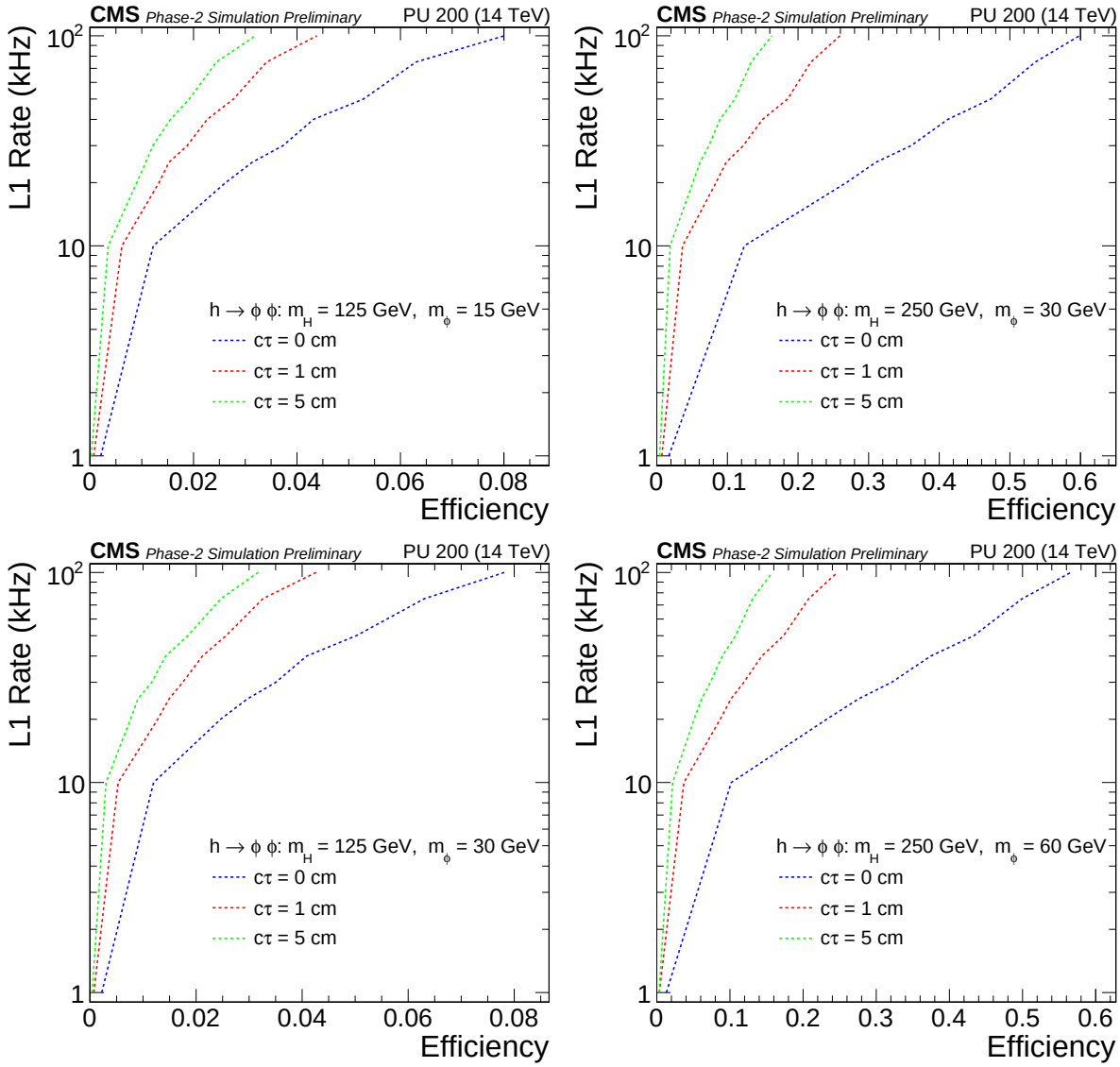

Figure 6: The rate of the track jet H_T trigger as a function of signal efficiency for the SM-like Higgs boson (left) and the heavy SM-like Higgs boson (right) using prompt track finding.

that requires a jet with a displaced tag make the signals with low H_T accessible for displaced jets.

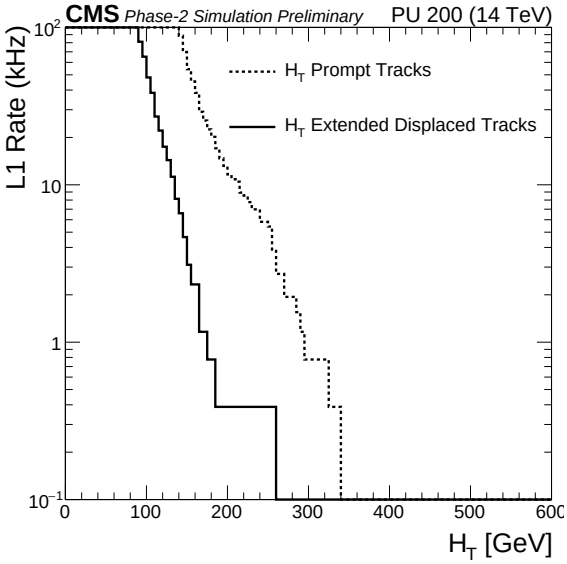

Figure 7: The rate of the track jet H_T trigger using extended track finding with (solid line) and without (dashed line) a requirement of at least one jet with a displaced tag.

In order to compare the results with prompt and extended track reconstruction, one needs to make a correction for the rapidity coverage: prompt tracks are found in $|\eta| < 2.4$, while the extended track algorithm currently only reconstructs tracks in $|\eta| < 1.0$. For the feasible thresholds, the rate for $|\eta| < 0.8$ and $|\eta| < 2.4$ differ by a factor of five. To scale the efficiency for finding track jets to the full $|\eta| < 2.4$ range, we derive a scale factor (SF) based on efficiency in the full η range and the central η range. The signal efficiency SFs range from 4–6, which is comparable to the increase in the L1 rate. We have confirmed that such extrapolation works for the track jets clustered with prompt tracks. Figure 8 shows the expected trigger rate as a function of efficiency for the SM and the heavy SM-like Higgs bosons.

5.3 Expected event yields

The available bandwith for the triggers described above, if implemented, will be decided as a part of the full trigger menu optimization. Here, we consider two cases, 5 and 25 kHz. The expected event yield for triggers using extended and prompt tracking are shown in Fig. 9, assuming branching fraction $\mathcal{B}[\mathrm{H}(125) \to \phi\phi \to 4j] = 10^{-5}$ for the SM-like Higgs boson. For the heavy Higgs boson, the expected number of produced signal events is set to be the same as for the SM-like Higgs by requiring $\sigma_{\mathrm{pp}\to\mathrm{H}(250)}\mathcal{B}[\mathrm{H}(250) \to \phi\phi \to 4j] = 10^{-5}\sigma_{\mathrm{pp}\to\mathrm{H}(125)}$.

6 Conclusion

We have studied the upgraded CMS detector's ability to trigger on events with long lived particles decaying into jets. Currently, such events pass the L1 trigger only if the total transverse energy in the event is above a few hundred GeV. This is an important blind spot for searches, especially for the rare exotic Higgs boson decays like $\mathrm{H}(125) \to \phi\phi \to 4j$.

In this note, a new L1 trigger strategy based on the Phase-2 CMS detector's ability to find tracks at L1 is explored. Using L1 tracks for jet reconstruction significantly suppresses pile-up and

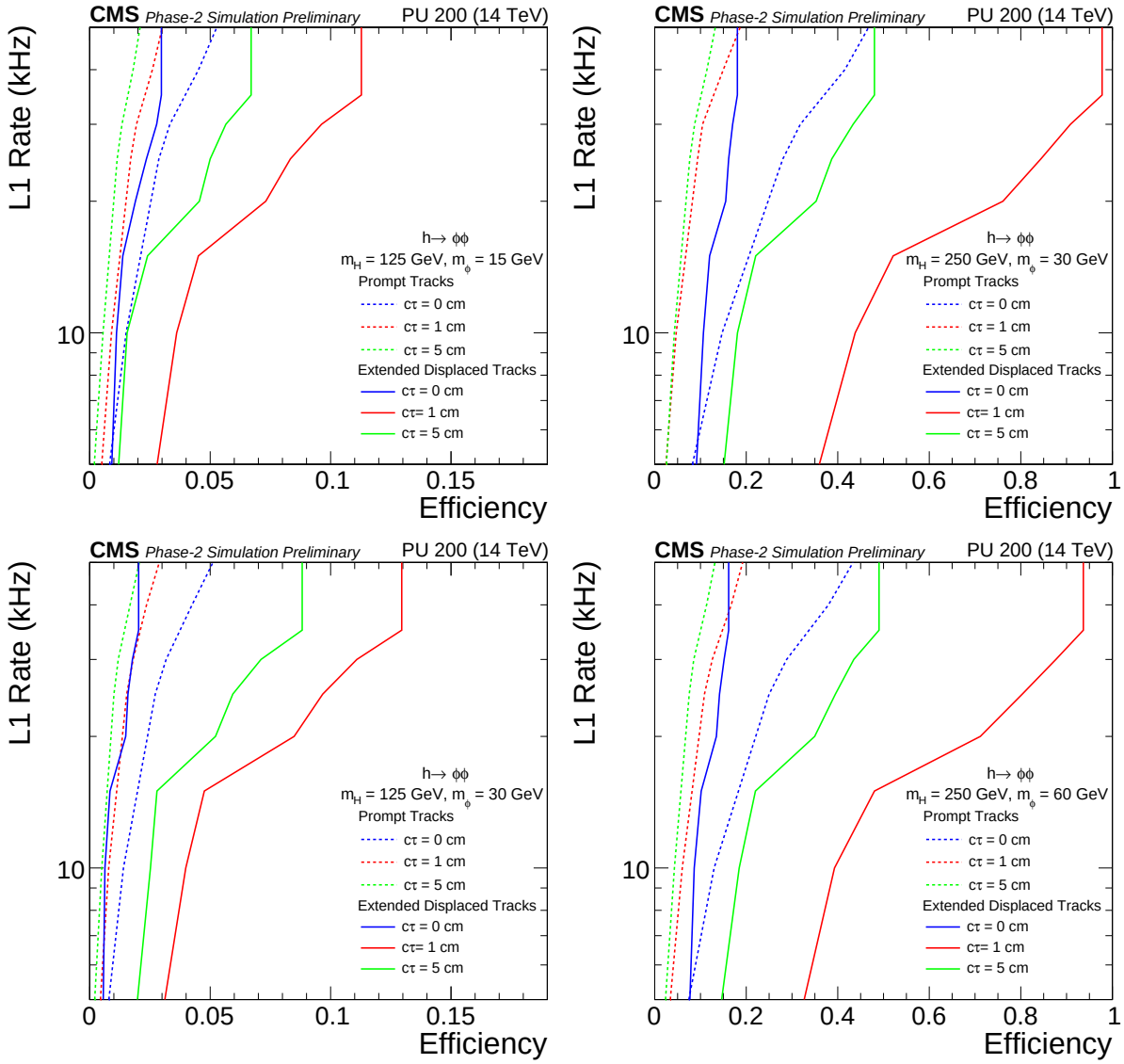

Figure 8: The rate of the track jet H_T trigger as a function of signal efficiency using extended track finding for the SM-like Higgs (left) and the heavy SM-like Higgs (right). The extended track finding performance is extrapolated to the full outer tracker acceptance as described in text.

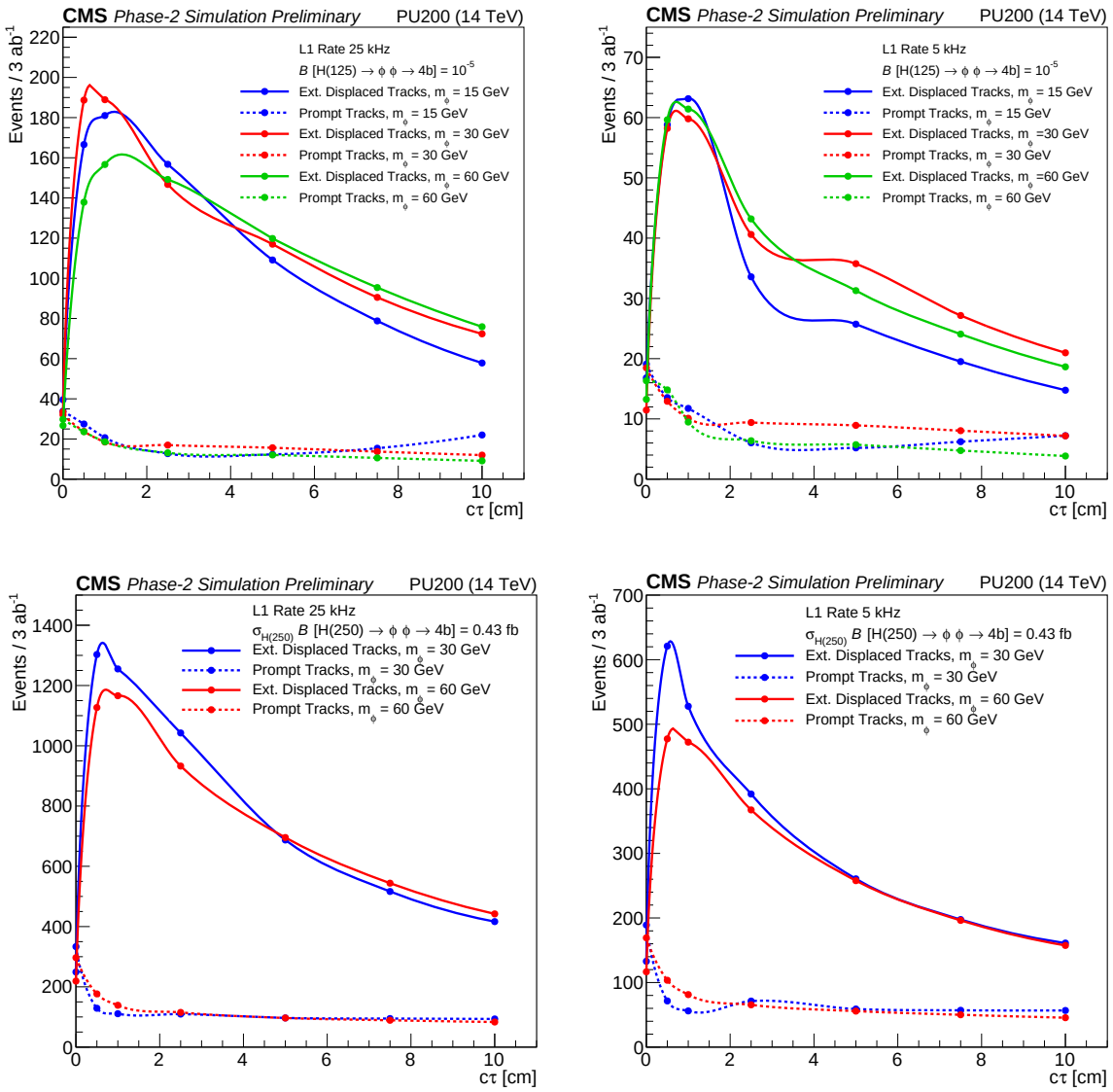

Figure 9: This plot shows the number of triggered Higgs events (assuming $\mathcal{B}[\mathrm{H}(125) \to \phi\phi \to 4j] = 10^{-5}$, corresponding to 1700 events) as a function of $c\tau$ for two choices for the trigger rates: 25 kHz (left), 5 kHz (right). Two triggers are compared: one based on prompt track finding (dotted lines) and another that is based on extended track finding with a displaced jet tag (solid lines).

allows to accept events with lower H_T. For the exotic Higgs decays considered, given the total Phase-2 dataset of $3\,\text{ab}^{-1}$ and branching fraction of 10^{-5}, CMS would collect $\mathcal{O}(10)$ events, which should be sufficient for discovery. We also considered a plausible extension of the L1 track finder to consider tracks with impact parameters of a few cm. That approach improves the yield by more than an order of magnitude. The gains for the extended L1 track finding are even larger for the events with larger H_T, as demonstrated by the simulations of heavy Higgs boson decays.

References

[1] CMS Collaboration, "The Phase-2 Upgrade of the CMS Tracker", CMS Technical Design Report CERN-LHCC-2017-009, CMS-TDR-014, CERN, 2017.

[2] CMS Collaboration, "The Phase-2 Upgrade of the CMS Barrel Calorimeter", CMS Technical Design Report CERN-LHCC-2017-011, CMS-TDR-015, CERN, 2017.

[3] CMS Collaboration, "The Phase-2 Upgrade of the CMS Endcap Calorimeter", CMS Technical Design Report CERN-LHCC-2017-023, CMS-TDR-019, CERN, 2017.

[4] CMS Collaboration, "The Phase-2 Upgrade of the CMS Muon Detectors", CMS Technical Design Report CERN-LHCC-2017-012, CMS-TDR-016, CERN, 2017.

[5] CMS Collaboration, "The Phase-2 Upgrade of the CMS L1 Trigger Interim Technical Design Report", CMS Technical Design Report CERN-LHCC-2017-013, CMS-TDR-017, CERN, 2017.

[6] CMS Collaboration, "Search for long-lived particles with displaced vertices in multijet events in pp collision events at $\sqrt{s} = 13\,\text{TeV}$", (2018). arXiv:1808.03078. Submitted to *Phys. Rev. D*.

[7] ATLAS Collaboration, "Search for the Higgs boson produced in association with a vector boson and decaying into two spin-zero particles in the $H \to aa \to 4b$ channel in pp collisions at $\sqrt{s} = 13$ TeV with the ATLAS detector", *JHEP* **10** (2018) 031, doi:10.1007/JHEP10(2018)031, arXiv:1806.07355.

[8] CMS Collaboration, "Search for new long-lived particles at $\sqrt{s} = 13\,\text{TeV}$", *Phys. Lett. B* **780** (2017) 432, doi:10.1016/j.physletb.2018.03.019.

[9] D. Curtin et al., "Exotic decays of the 125 GeV Higgs boson", *Phys. Rev. D* **90** (2014) 075004, doi:10.1103/PhysRevD.90.075004, arXiv:1312.4992.

[10] GEANT4 Collaboration, "GEANT4—a simulation toolkit", *Nucl. Instrum. Meth. A* **506** (2003) 250, doi:10.1016/S0168-9002(03)01368-8.

[11] S. Alioli, P. Nason, C. Oleari, and E. Re, "NLO Higgs boson production via gluon fusion matched with shower in POWHEG", *JHEP* **04** (2009) 002, doi:10.1088/1126-6708/2009/04/002, arXiv:0812.0578.

[12] T. Sjöstrand et al., "An Introduction to PYTHIA 8.2", *Comput. Phys. Commun.* **191** (2015) 159–177, doi:10.1016/j.cpc.2015.01.024, arXiv:1410.3012.

[13] M. Cacciari, G. P. Salam, and G. Soyez, "The anti-k_T jet clustering algorithm", *JHEP* **04** (2008) 063, doi:10.1088/1126-6708/2008/04/063, arXiv:0802.1189.

[14] M. Cacciari, G. P. Salam, and G. Soyez, "FastJet User Manual", *Eur. Phys. J. C* **72** (2012) 1896, doi:10.1140/epjc/s10052-012-1896-2, arXiv:1111.6097.